

Impact of the SiO₂ interface layer on the crystallographic texture of ferroelectric hafnium oxide ^{EP}

Cite as: Appl. Phys. Lett. **118**, 012901 (2021); <https://doi.org/10.1063/5.0029635>

Submitted: 15 September 2020 • Accepted: 19 December 2020 • Published Online: 04 January 2021

 M. Lederer,  A. Reck, K. Mertens, et al.

COLLECTIONS

Paper published as part of the special topic on [Ferroelectricity in Hafnium Oxide: Materials and Devices](#)

 This paper was selected as an Editor's Pick



View Online



Export Citation



CrossMark

ARTICLES YOU MAY BE INTERESTED IN

[Polarization switching in thin doped HfO₂ ferroelectric layers](#)

Applied Physics Letters **117**, 262904 (2020); <https://doi.org/10.1063/5.0035100>

[Ferroelectricity in hafnium oxide thin films](#)

Applied Physics Letters **99**, 102903 (2011); <https://doi.org/10.1063/1.3634052>

[Next generation ferroelectric materials for semiconductor process integration and their applications](#)

Journal of Applied Physics **129**, 100901 (2021); <https://doi.org/10.1063/5.0037617>

 QBLOX



1 qubit

Shorten Setup Time

Auto-Calibration
More Qubits

Fully-integrated

Quantum Control Stacks
Ultrastable DC to 18.5 GHz
Synchronized <<1 ns
Ultralow noise



100s qubits

[visit our website >](#)

Impact of the SiO₂ interface layer on the crystallographic texture of ferroelectric hafnium oxide

Cite as: Appl. Phys. Lett. **118**, 012901 (2021); doi: [10.1063/5.0029635](https://doi.org/10.1063/5.0029635)

Submitted: 15 September 2020 · Accepted: 19 December 2020 ·

Published Online: 4 January 2021








View Online



Export Citation



CrossMark

M. Lederer,^{1,a)}  A. Reck,¹  K. Mertens,¹ R. Olivo,¹ P. Bagul,¹  A. Kia,¹ B. Volkmann,² T. Kämpfe,¹  K. Seidel,¹ and L. M. Eng³ 

AFFILIATIONS

¹Fraunhofer IPMS, Königsbrücker Str. 178, 01099 Dresden, Germany

²GLOBALFOUNDRIES Fab 1 LLC & Co. KG, Dresden 01109, Germany

³Institut für Angewandte Physik, Technische Universität Dresden, 01069 Dresden, Germany

Note: This paper is part of the Special Topic on Materials and Devices Utilizing Ferroelectricity in Hafnium Oxide.

^{a)}Author to whom correspondence should be addressed: maximilian.lederer@ipms.fraunhofer.de

ABSTRACT

Applying transmission Kikuchi diffraction (TKD) allows us to fundamentally investigate the Si-doped-hafnium-oxide (HSO) microstructure that results from the interface layer present in ferroelectric field-effect transistors. In addition to the predominant orthorhombic phase, dendritic HSO grains larger than 100 nm govern the microstructure composition. Furthermore, the observed strong out-of-plane texture aligned along the [110] and [011] axis clearly differs from features found in hafnium oxide thin films grown on TiN layers. Our TKD analysis shows that the texture intensity strongly varies for samples annealed at different temperatures. Additionally, intra-granular misorientation and chemical composition analyses of the layers provide insight into the crystallization process of these ferroelectric thin films.

© 2021 Author(s). All article content, except where otherwise noted, is licensed under a Creative Commons Attribution (CC BY) license (<http://creativecommons.org/licenses/by/4.0/>). <https://doi.org/10.1063/5.0029635>

Transmission Kikuchi diffraction (TKD) enables the microstructure analysis of ultra-thin films, including local crystallographic phase and orientation mapping.^{1,2} This method recently has been beautifully demonstrated as a powerful tool for ferroelectric hafnium oxide analysis,³ which certainly spurs research interest in a broad range of applications, e.g., nonvolatile memories or pyroelectric sensors.^{4,5}

Ferroelectricity in hafnium oxide has been demonstrated to originate from the orthorhombic phase with space group $Pca2_1$.⁶ This metastable phase can be stabilized, e.g., by doping^{7,8} or when applying mechanical stress due to the presence of a capping layer.⁹ Nevertheless, the microstructure may contain grains of other polymorphs like the monoclinic ($P2_1/c$) phase, which represents the thermodynamic ground state.¹⁰

The large coercive field, superior thickness scaling below the 5 nm threshold, and complementary-metal-oxide-semiconductor (CMOS) process compatibility for ferroelectric HfO₂ make these thin films superior to classical perovskite-based ferroelectrics such as lead titanate zirconate, for instance, in nonvolatile memory applications.¹¹ More specifically, this already enabled realizing one-transistor

(1T)-based ferroelectric memories, namely, ferroelectric field-effect transistors (FeFETs).¹² Compared to capacitor-based memory concepts where the ferroelectric is located between two metallic electrodes, preferably TiN, HfO₂ in FeFETs is introduced directly into the gate stack with the HfO₂ typically being sandwiched in-between the bottom SiO₂ interface layer (covering the semiconductor surface) and the top TiN electrode. FeFETs structured in this manner were already integrated into the 28 nm and 22 nm node technology.^{13,14}

For investigating how this interface layer impacts the crystallization process and, therefore, the microstructure, we analyze here Si-doped hafnium oxide (HSO) layers in the aforementioned layer stack annealed at different temperatures using TKD. All samples are produced by atomic layer deposition (ALD) of HSO onto highly p-doped Si wafers covered with a native oxide layer. Here, HfCl₄ and SiCl₄ are used as precursors in a cycle ratio of 16:1. Electrodes are formed via physical vapor deposition of TiN. The crystallization anneal is performed by rapid thermal processing at 650 °C, 800 °C, and 1000 °C.

TKD measurements on dimpled samples are carried out using a Bruker Optimus TKD detector head mounted into a scanning electron

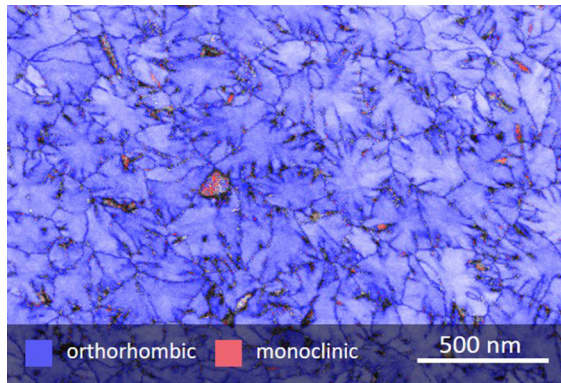


FIG. 1. Microstructure and crystallographic phase distribution of the Si-doped hafnium oxide layer annealed at 650 °C. Most grains are of dendritic shape in the orthorhombic phase (blue color), while only a small amount of monoclinic grains is found (red). Note that the tetragonal, cubic, and rhombohedral phases were not analyzed here.

microscope. The acceleration voltage is 30 kV and a current of 3.2 nA is used. The details on the measurement method and data processing have been shown in a previous work.³ Additionally, grazing-incident X-ray diffraction (GIXRD) measurements were performed with 2θ ranging from 15° to 45° in 0.1° steps. The chemical composition of the films is analyzed with time-of-flight secondary-ion-mass spectrometry (ToF-SIMS). Capacitor structures were formed by shadow-mask-based deposition of Ti/Pt contacts and subsequent wet etch.

The grain structure of the HSO layers appears very clearly in the quality/phase map, as depicted in Fig. 1 for the HSO sample annealed at 650 °C. As seen, the orthorhombic phase (blue color) dominates, with some residual grains being monoclinic (red color). Note that the tetragonal phase has not been taken into account, since the Curie temperature lies between 250 °C and 500 °C.^{16–18} Furthermore, cubic and rhombohedral phases were excluded since being less stable than the orthorhombic phase, as theoretically backed up by density functional theory.^{10,19,20} Furthermore, initial dynamic hysteresis measurements on pristine capacitor structures revealed ferroelectric behavior with high polarization values [see Fig. 2(a)]. In contrast to the previously reported microstructures of HSO and Zr-doped hafnium oxide (HZO)

metal–ferroelectric–metal (MFM) structures^{3,15} finding disc-shaped columnar grains, dendritic grains are detected here in the metal–ferroelectric–insulator–semiconductor (MFIS) structures.

In addition to a value of 52 nm, the average equivalent grain size of MFM samples weighted by area¹⁵ is significantly smaller than the one measured for the MFIS samples, having values between 232 nm and 244 nm [see Fig. 2(b)]. Since both MFM and MFIS samples were annealed under similar conditions, the observed strong differences in precipitation must be clearly related to the substrate layer in use, i.e., the amorphous SiO₂ and the polycrystalline ALD TiN layer with a slight (111) texture.²¹ Consequently, various effects might impact the crystallization behavior, such as changes in the local mechanical stress field resulting from different thermal expansion coefficients of the materials, or variation in the nucleation behavior, e.g., heterogeneous and homogeneous nucleation. Bagmut *et al.* stated that the onset of crystalline phase formation in HfO₂ initiates at higher temperature when using amorphous substrates instead of (poly)crystalline ones.²² In addition, island (IPC) and dendrite (DPC) polymorphic growth were reported for zirconium and hafnium oxides, with IPC or DPC nucleating in the cubic/tetragonal or orthorhombic/monoclinic phase, respectively.^{22–24}

When comparing samples that have been annealed at different temperatures, the average grain size remains constant and no clear trend with temperature is observed. This is quite remarkable, as crystal growth generally is very temperature sensitive due to on-surface diffusion. Notably, monoclinic grains show this temperature dependence, and their fraction grows with increasing temperature [see Fig. 2(c)]. In samples annealed at 650 °C, only a low number of grains is monoclinic (see Fig. 1), with this fraction significantly growing for elevated annealing temperatures. This is exactly seen from Fig. 2(c) when plotting the equivalent grain diameter vs annealing temperature.

A possible explanation for this behavior is the phase transformation of amorphous HfO₂ reported by Bagmut,²⁴ which proceeds in two steps: first, orthorhombic grains grow up to a critical grain diameter D^* above which they transform into the monoclinic phase. The reported values for D^* range from 143 nm to 294 nm (Ref. 24) and are comparable to the average grain sizes reported in this work here. As the transition to the monoclinic phase involves unit-cell shearing (that, notably, is mechanically suppressed when using TiN capping layers⁷) we believe that this phase transition in MFIS structures is shifted to higher temperatures, with some larger grains already being

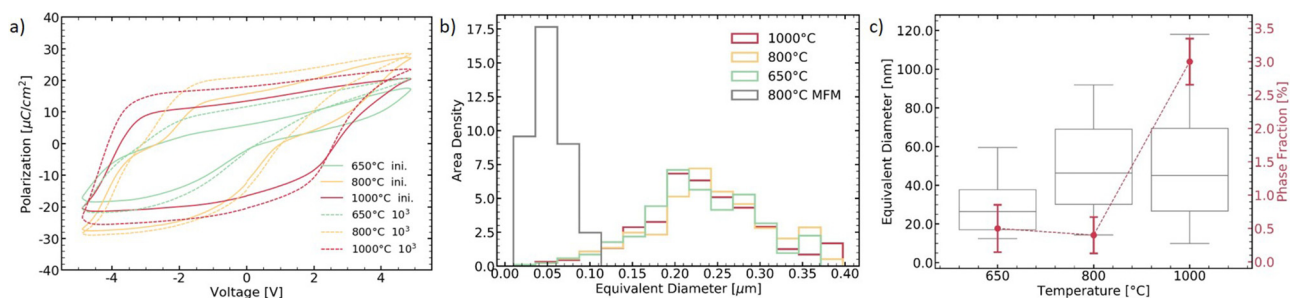


FIG. 2. Polarization response and grain size distribution of HSO in MFIS structures annealed at different temperatures: (a) ferroelectric behavior observed by dynamic hysteresis measurements with an amplitude of 5 V at 1 kHz for the pristine and cycled film. Electric field cycling is performed under identical conditions. (b) The distribution of the equivalent diameter, weighted by area, shows a strong increase in grain size for MFIS samples as compared to the HSO MFM sample (as reported earlier¹⁵). The annealing temperature seems to have no impact on the grain size; (c) both the extracted equivalent grain diameter in the monoclinic phase and the monoclinic phase fraction increase with elevated annealing temperature.

TABLE I. Crystallographic texture, grain size, and shape of HSO-based MFM and MFIS structures, respectively.

Substrate	Ferroelectric	Anneal	Average grain size (weighted by area)	Grain shape	Out-of-plane texture
ALD TiN, polycrystalline, (111) texture ²¹	ALD HSO 10 nm (Ref. 15)	800 °C (Ref. 15)	52 nm (Ref. 15)	Disc-shaped ¹⁵	[010] ¹⁵
SiO ₂ , amorphous	ALD HSO 10 nm	650 °C–1000 °C	232 nm–244 nm	Dendritic	[110] and [011]

rendered monoclinic. In addition to the two-stage process, the nucleation of the monoclinic phase has been demonstrated experimentally as well²⁴ and may also explain the small monoclinic grains present in all samples here.

The strong differences in the HSO microstructure for MFM and MFIS samples (as summarized in Table I) are further underlined when analyzing their crystallographic texture. While an out-of-plane texture of the [002]- and [020]-axis was reported for HSO and HZO MFM samples,^{3,15,25} a different texture is observed on the MFIS stacks. As shown with the inverse pole figure (IPF) maps in Fig. 3(a), MFIS samples annealed at 1000 °C indicate a clear out-of-plane texture as well. Some grains aligned closely to the [010]- or [001]-axis appear with dots or larger connected regions of the [001]- or [010]-axis, respectively, a signature that can be easily assigned to either misindexing or ferroelasticity, as these are the axes that most likely undergo ferroelastic switching.²⁶

For a detailed analysis of the out-of-plane texture, pole figures are extracted [see Fig. 3(b)]. Here, the [010]-axis does not align parallel but rather donut-shaped around the out-of-plane axis

of the sample. Instead, the [110]- and [011]-axis align parallel to this axis. Furthermore, the [111]-axis shows a weak texture aligning either parallel or perpendicular to the normal vector of the thin film. This would result in a tilted polarization axis after wake-up and, therefore, in an increase in the effective coercive field of the layer. A similar orientation of the polarization axis has also been reported for a 22-nm FeFET.¹⁵

With decreasing annealing temperature, this texture becomes less dominant while more [111]- and [101]-axes align out-of-plane [see Fig. 3(c)]. This agrees well with the measured GIXRD patterns [see Fig. 3(d)], where an increased intensity of the diffraction line at 24°, corresponding to the (110) index, is observed for the 1000 °C anneal. Minor shifts of the diffraction lines to higher angles are likely to originate from strain inside the layer. Nevertheless, a texture that might be described by a preferred absence of all <100> axes is very surprising for a layer grown on an amorphous substrate, as no orientational information can be transferred to the hafnium oxide. Moreover, the polymorphic phase transitions that HfO₂ is likely to undergo would not enable the formation of such a texture.

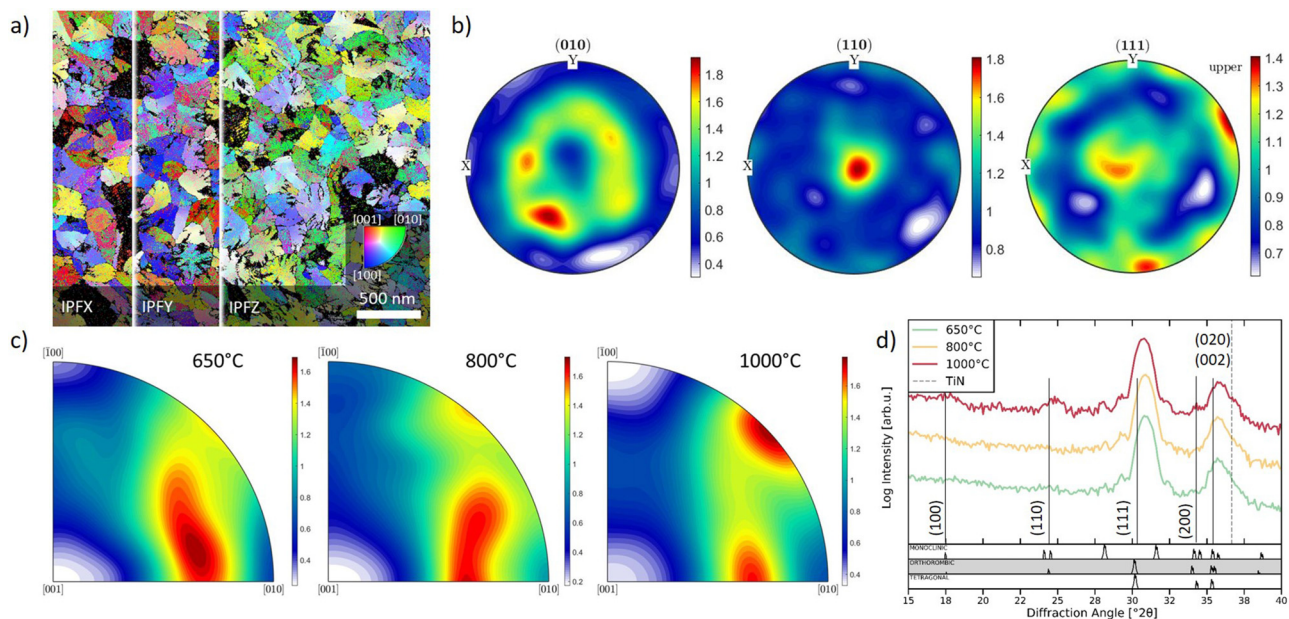


FIG. 3. TKD microstructure analysis: (a) inverse pole figure maps of the x, y, and z planes for the sample annealed at 1000 °C highlight the presence of an out-of-plane texture; (b) pole figures of the same sample indicate the sample normal vector to be [110] aligned; (c) inverse pole figures of the z plane show an increasing texture along the [110] and [011] axes when raising the annealing temperature. Samples annealed at lower temperature also show [111]- and [101]-axis alignment; and (d) accompanying GIXRD patterns supporting our TKD results.

In addition to the reported textures, intra-granular orientational shifts can be deduced from the IPF maps [see Fig. 3(a)] in the form of color gradients. In order to remove misindexing or ferroelastic contributions, cubic symmetry operations are applied to highlight these gradients [see Fig. 4(a)]. When calculating the mean orientation of every grain, intra-granular misorientation can be visualized. As shown in Fig. 4(b), the misorientation is especially high in the dendrites. As this correlates with increased stress and defect level, it is very likely to assume that the interplay of ferroelectric and ferroelastic switching will differ in these regions. Note that beyond such local stress fields, the thermal expansion mismatch between adjacent layers will equally impact the ferroelectric switching behavior.

As the presence of diffusion cannot be ruled out for the annealing temperatures used here, the chemical composition of the layer stack is investigated as well using time-of-flight secondary-ion-mass spectrometry (ToF-SIMS). When mapping the area-integrated signal intensity of selected molecular ions, oxidation at both interfaces of the TiN layers is observed for samples annealed at 650 °C and 1000 °C, respectively. Moreover, the SiO₂ interface layer shows accumulation of nitrogen when annealing at 1000 °C, indicating diffusion of nitrogen through the HSO layer [see Fig. 5(a)]. Furthermore, an increase in the interfacial layer thickness is observed. This increase is also present in the HfSiO₄⁻ signal, suggesting the presence of hafnium or the formation of hafnon (HfSiO₄) in

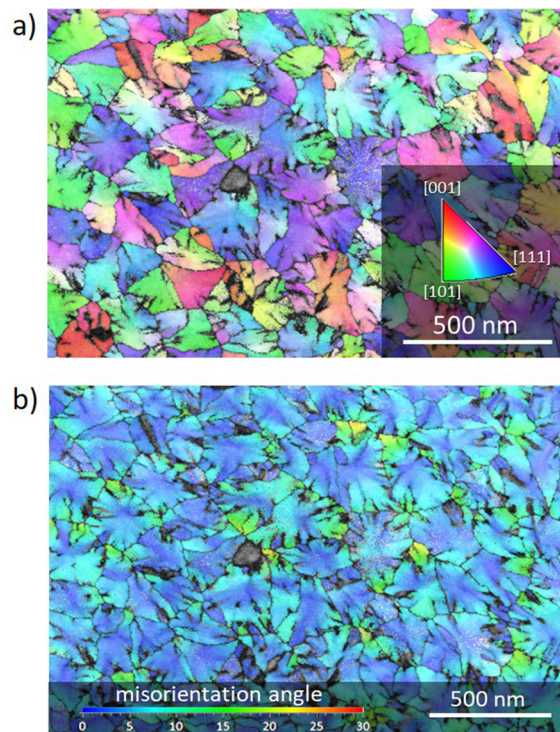


FIG. 4. Extraction of intragranular misorientation: (a) under the assumption of higher (cubic) symmetry, 90°-angle based misindexing and ferroelastic components disappear, but lattice distortions remain, as shown for the sample annealed at 650 °C; (b) this allows calculating the intra-granular misorientation angle with respect to the mean orientation, showing strong distortions for dendrites.

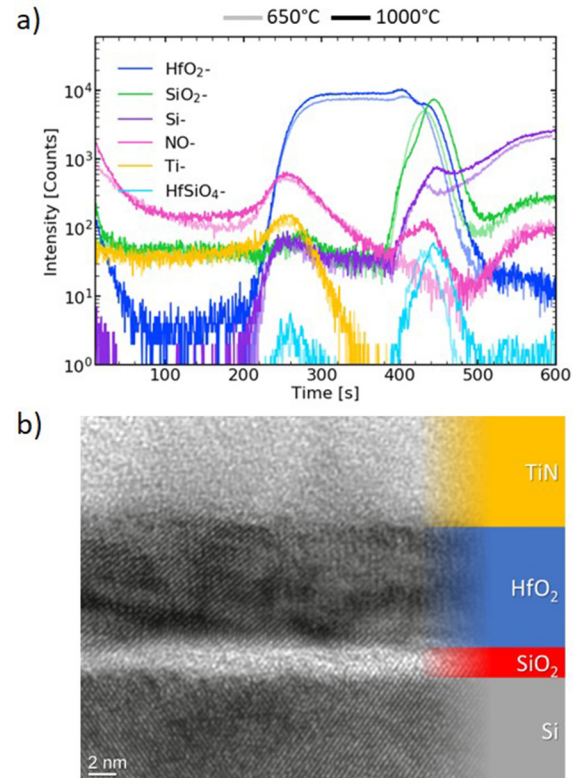


FIG. 5. Chemical and structural analysis of the adjacent layers: (a) the ToF-SIMS depth profile indicates both nitrogen accumulation in and thickness growth of the interface layer for elevated annealing temperatures; (b) TEM analysis confirms the amorphous structure of the interface layer for all annealing temperatures used.

the interface layer during the anneal process. Nevertheless, the SiO₂ interface layer still is amorphous as confirmed by transmission electron microscopy [see Fig. 5(b)]. Consequently, the crystallization anneal of Si-doped hafnium oxide on an interface layer is characterized by the subtle interplay of diffusion and crystallization processes. As mentioned above, diffusion alone cannot explain the observed textures, as the interface layer remains amorphous.

In conclusion, TKD measurements of Si-doped hafnium oxide layers grown on silicon oxide reveal a microstructure dominated by dendritic orthorhombic grains, having an average equivalent diameter of about 230 nm for annealing temperatures ranging from 650 °C to 1000 °C. Additionally, a strong [110] and [011] out-of-plane texture is found that becomes more prominent with increasing annealing temperatures. This strongly contrasts HfO₂ layers grown on polycrystalline TiN layers, which have a significantly smaller grain size and show considerable [020] or [002] out-of-plane textures.^{3,15} Misorientation analysis highlights the strong mechanically induced distortions observed for dendrites, while ToF-SIMS measurements indicate both an increased thickness and nitrogen concentration of interface layers. MFIS structures, hence, show a fundamentally altered interface morphology and texture compared to MFM samples, with a clear impact on their ferroelectric switching behavior.

We kindly acknowledge financial support for the work presented here by the German Bundesministerium für Wirtschaft (BMWi) and by the State of Saxony in the frame of the Important Project of Common European Interest (IPCEI) as well as by the German Federal Ministry of Education and Research under the project Reference Nos. 16FMD01K, 16FMD02, and 16FMD03.

DATA AVAILABILITY

The data that support the findings of this study are available from the corresponding author upon reasonable request.

REFERENCES

- ¹R. R. Keller and R. H. Geiss, "Transmission EBSD from 10 nm domains in a scanning electron microscope," *J. Microsc.* **245**, 245–251 (2012).
- ²P. W. Trimby, "Orientation mapping of nanostructured materials using transmission Kikuchi diffraction in the scanning electron microscope," *Ultramicroscopy* **120**, 16–24 (2012).
- ³M. Lederer, T. Kämpfe, R. Olivo, D. Lehninger, C. Mart, S. Kirbach, T. Ali, P. Polakowski, L. Roy, and K. Seidel, "Local crystallographic phase detection and texture mapping in ferroelectric Zr doped HfO₂ films by transmission-EBSD," *Appl. Phys. Lett.* **115**, 222902 (2019).
- ⁴T. Mikolajick, U. Schroeder, S. Slesazek, and T. Mikolajick, "The past, the present, and the future of ferroelectric memories," *IEEE Trans. Electron Devices* **67**, 1434–1410 (2020).
- ⁵C. Mart, T. Kämpfe, S. Zybelle, and W. Weinreich, "Layer thickness scaling and wake-up effect of pyroelectric response in Si-doped HfO₂," *Appl. Phys. Lett.* **112**, 052905 (2018).
- ⁶X. Sang, E. D. Grimley, T. Schenk, U. Schroeder, and J. M. LeBeau, "On the structural origins of ferroelectricity in HfO₂ thin films," *Appl. Phys. Lett.* **106**, 162905 (2015).
- ⁷T. S. Böske, J. Müller, D. Bräuhaus, U. Schröder, and U. Böttger, "Ferroelectricity in hafnium oxide thin films," *Appl. Phys. Lett.* **99**, 102903 (2011).
- ⁸J. Müller, T. S. Böske, U. Schröder, S. Müller, D. Bräuhaus, U. Böttger, L. Frey, and T. Mikolajick, "Ferroelectricity in simple binary ZrO₂ and HfO₂," *Nano Lett.* **12**, 4318–4323 (2012).
- ⁹P. Polakowski and J. Müller, "Ferroelectricity in undoped hafnium oxide," *Appl. Phys. Lett.* **106**, 232905 (2015).
- ¹⁰R. Materlik, C. Künneth, and A. Kersch, "The origin of ferroelectricity in Hf_{1-x}Zr_xO₂: A computational investigation and a surface energy model," *J. Appl. Phys.* **117**, 134109 (2015).
- ¹¹J. Müller, P. Polakowski, S. Müller, and T. Mikolajick, "Ferroelectric hafnium oxide based materials and devices: Assessment of current status and future prospects," *ECS J. Solid State Sci. Technol.* **4**, N30–N35 (2015).
- ¹²N. Gong and T.-P. Ma, "Why is FE-HfO₂ more suitable than PZT or SBT for scaled nonvolatile 1-T memory cell? A retention perspective," *IEEE Electron Device Lett.* **37**, 1123–1126 (2016).
- ¹³J. Müller, E. Yurchuk, T. Schlosser, J. Paul, R. Hoffmann, S. Müller, D. Martin, S. Slesazek, P. Polakowski, J. Sundqvist, M. Czernohorsky, K. Seidel, P. Kucher, R. Boschke, M. Trentzsch, K. Gebauer, U. Schroeder, and T. Mikolajick, "Ferroelectricity in HfO₂ enables nonvolatile data storage in 28 nm HKMG," in *Symposium on VLSI Technology, VLSI (IEEE, Honolulu, HI, USA, 2012)*, pp. 25–26.
- ¹⁴S. Dünkel, M. Trentzsch, R. Richter, P. Moll, C. Fuchs, O. Gehring, M. Majer, S. Wittek, B. Müller, T. Melde, H. Mulaosmanovic, S. Slesazek, S. Müller, J. Ocker, M. Noack, D.-A. Lohr, P. Polakowski, J. Müller, T. Mikolajick, J. Hontschel, B. Rice, J. Pellerin, and S. Beyer, "A FeFET based super-low-power ultra-fast embedded NVM technology for 22 nm FDSOI and beyond," in *IEEE International Electron Devices Meeting, IEDM (IEEE, San Francisco, CA, USA, 2017)*, pp. 19.7.1–19.7.4.
- ¹⁵M. W. Lederer, T. Kämpfe, N. Vogel, D. Utesch, B. Volkmann, T. Ali, R. Olivo, J. Müller, S. Beyer, M. Trentzsch, K. Seidel, and L. M. Eng, "Structural and electrical comparison of Si and Zr doped hafnium oxide thin films and integrated FeFETs utilizing transmission Kikuchi diffraction," *Nanomaterials* **10**, 384 (2020).
- ¹⁶M. Hoffmann, U. Schroeder, C. Künneth, A. Kersch, S. Starschich, U. Böttger, and T. Mikolajick, "Ferroelectric phase transitions in nanoscale HfO₂ films enable giant pyroelectric energy conversion and highly efficient supercapacitors," *Nano Energy* **18**, 154–164 (2015).
- ¹⁷T. Nishimura, L. Xu, S. Shibayama, T. Yajima, S. Migita, and A. Toriumi, "Ferroelectricity of nondoped thin HfO₂ films in TiN/HfO₂/TiN stacks," *Jpn. J. Appl. Phys., Part 1* **55**, 08PB01 (2016).
- ¹⁸T. Mimura, T. Shimizu, Y. Katsuya, O. Sakata, and H. Funakubo, "Thickness- and orientation- dependences of Curie temperature in ferroelectric epitaxial Y doped HfO₂ films," *Jpn. J. Appl. Phys., Part 1* **59**, SGG04 (2020).
- ¹⁹Y. Wei, P. Nukala, M. Salverda, S. Matzen, H. J. Zhao, J. Momand, A. S. Everhardt, G. Agnus, G. R. Blake, P. Lecoeur, B. J. Kooi, J. Íñiguez, B. Dkhil, and B. Noheda, "A rhombohedral ferroelectric phase in epitaxially strained Hf_{0.5}Zr_{0.5}O₂ thin films," *Nat. Mater.* **17**, 1095–1100 (2018).
- ²⁰C. Künneth, R. Materlik, M. Falkowski, and A. Kersch, "Impact of four-valent doping on the crystallographic phase formation for ferroelectric HfO₂ from first-principles: Implications for ferroelectric memory and energy-related applications," *ACS Appl. Nano Mater.* **1**, 254–264 (2018).
- ²¹J. Speulmanns, A. M. Kia, K. Kühnel, S. Bönhardt, and W. Weinreich, "Surface-dependent performance of ultrathin TiN films as an electrically conducting Li diffusion barrier for Li-ion-based devices," *ACS Appl. Mater. Interfaces* **12**, 39252–39260 (2020).
- ²²A. G. Bagmut, I. A. Bagmut, V. A. Zhuchkov, and M. O. Shevchenko, "Phase transformations in films deposited by laser ablation of Hf in an oxygen atmosphere," *Tech. Phys.* **57**, 856–860 (2012).
- ²³A. G. Bagmut and I. A. Bagmut, "Structure and kinetics of the crystallization of oxide films, deposited by laser ablation," in *2017 IEEE 7th International Conference Nanomaterials: Application & Properties (NAP) (IEEE, Odessa, 2017)*, pp. 02NTF14-1–02NTF14-4.
- ²⁴A. G. Bagmut, "Kinetics of crystals growth under electron-beam crystallization of amorphous films of hafnium dioxide," *Funct. Mater.* **25**, 525–533 (2018).
- ²⁵T. Schenk, C. M. Fancher, M. H. Park, C. Richter, C. Künneth, A. Kersch, J. L. Jones, T. Mikolajick, and U. Schroeder, "On the origin of the large remanent polarization in La:HfO₂," *Adv. Electron. Mater.* **5**, 1900303 (2019).
- ²⁶T. Shimizu, T. Mimura, T. Kiguchi, T. Shiraishi, T. J. Konno, Y. Katsuya, O. Sakata, and H. Funakubo, "Ferroelectricity mediated by ferroelastic domain switching in HfO₂-based epitaxial thin films," *Appl. Phys. Lett.* **113**, 212901 (2018).